In vitro and in vivo evaluation of Δ9-tetrahidrocannabinol/PLGA nanoparticles for cancer chemotherapy

ARTICLE *in* INTERNATIONAL JOURNAL OF PHARMACEUTICS · APRIL 2015

Impact Factor: 3.65 · DOI: 10.1016/j.ijpharm.2015.04.054 · Source: PubMed

10 AUTHORS, INCLUDING:

Lucia Martin-Banderas

Universidad de Sevilla

28 PUBLICATIONS **252** CITATIONS

SEE PROFILE

Inmaculada Muñoz

Ingeniatrics Technologies S.L.

6 PUBLICATIONS **24** CITATIONS

SEE PROFILE

Mr. Jose Manuel Calderon-Montaño

Universidad de Sevilla

5 PUBLICATIONS **113** CITATIONS

SEE PROFILE

Miguel López-Lázaro

Universidad de Sevilla

78 PUBLICATIONS **1,799** CITATIONS

SEE PROFILE

International Journal of Pharmaceutics 487 (2015) 205–212

Contents lists available at ScienceDirect

International Journal of Pharmaceutics

journal homepage: www.elsevier.com/locate/ijpharm

Pharmaceutical nanotechnology

In vitro and *in vivo* evaluation of Δ^9-tetrahidrocannabinol/PLGA nanoparticles for cancer chemotherapy

L. Martín-Banderas [a,*], I. Muñoz-Rubio [a], J. Prados [b,c], J. Álvarez-Fuentes [a], J.M. Calderón-Montaño [d], M. López-Lázaro [d], J.L. Arias [c,e], M.C. Leiva [b,c], M.A. Holgado [a], M. Fernández-Arévalo [a]

[a] Department of Pharmacy and Pharmaceutical Technology, Faculty of Pharmacy, University of Seville, Seville, Spain
[b] Institute of Biopathology and Regenerative Medicine (IBIMER), University of Granada, Granada, Spain
[c] Biosanitary Institute of Granada (ibs.GRANADA), Andalusian Health Service (SAS), University of Granada, Granada, Spain
[d] Department of Pharmacology, Faculty of Pharmacy, University of Seville, Seville, Spain
[e] Department of Pharmacy and Pharmaceutical Technology, Faculty of Pharmacy, University of Granada, Granada, Spain

ARTICLE INFO

Article history:
Received 24 February 2015
Received in revised form 15 April 2015
Accepted 16 April 2015
Available online 18 April 2015

Keywords:
Blood compatibility
Chitosan
Δ^9-Tetrahidrocannabinol
Lung cancer
Nanoparticles
PEGylation
PLGA

ABSTRACT

Nanoplatforms can optimize the efficacy and safety of chemotherapy, and thus cancer therapy. However, new approaches are encouraged in developing new nanomedicines against malignant cells. In this work, a reproducible methodology is described to prepare Δ^9-tetrahidrocannabinol (Δ^9-THC)-loaded poly(D,L-lactide-*co*-glycolide) (PLGA) nanoparticles against lung cancer. The nanoformulation is further improved by surface functionalization with the biodegradable polymers chitosan and poly(ethylene glycol) (PEG) in order to optimize the biological fate and antitumor effect. Mean nanoparticle size (≈290 nm) increased upon coating with PEG, CS, and PEG–CS up to ≈590 nm, ≈745 nm, and ≈790 nm, respectively. Surface electrical charge was controlled by the type of polymeric coating onto the PLGA particles. Drug entrapment efficiencies (≈95%) were not affected by any of the polymeric coatings. On the opposite, the characteristic sustained (biphasic) Δ^9-THC release from the particles can be accelerated or slowed down when using PEG or chitosan, respectively. Blood compatibility studies demonstrated the adequate *in vivo* safety margin of all of the PLGA-based nanoformulations, while protein adsorption investigations postulated the protective role of PEGylation against opsonization and plasma clearance. Cell viability studies comparing the activity of the nanoformulations against human A-549 and murine LL2 lung adenocarcinoma cells, and human embryo lung fibroblastic MRC-5 cells revealed a statistically significant selective cytotoxic effect toward the lung cancer cell lines. In addition, cytotoxicity assays in A-549 cells demonstrated the more intense anticancer activity of Δ^9-THC-loaded PEGylated PLGA nanoparticles. These promising results were confirmed by *in vivo* studies in LL2 lung tumor-bearing immunocompetent C57BL/6 mice.

1. Introduction

Δ^9-Tetrahidrocannabinol (Δ^9-THC) has attracted special interest in oncology given their well-known palliative effects and antitumor activity (Ramer and Hinz, 2008; Aviello et al., 2012; Velasco et al., 2012; Solinas et al., 2013). In fact, Δ^9-THC has been described to inhibit tumor angiogenesis and cell growth in malignant tissues, thus causing cell death (McKallip et al., 2002; Casanova et al., 2003; Blázquez et al., 2004; Bifulco et al., 2006; Ramer et al., 2012; Hernán Pérez de la Ossa et al., 2013a; Machado-Rocha et al., 2014).

Unfortunately, and despite oral aerosols, transdermal patches, and suppositories have been proposed (Hernán Pérez de la Ossa et al., 2013a), up to now the development of an effective and safety (Δ^9-THC)-based formulation remains to be accomplished. Probably, reasons beneath the challenge are the high instability, oily-resin nature, low water solubility (≈2.8 mg/L), and low bioavailability of the compound (Brownjohn and Ashton, 2012). To beat the challenge, (Δ^9-THC)-loaded microparticulate systems based on the polymer poly(ε-caprolactone) have been engineered by oil-in-water emulsion-solvent evaporation with promising results against cancer (Hernán Pérez de la Ossa et al., 2012,

* Corresponding author at: Departamento de Farmacia y Tecnología Farmacéutica, Facultad de Farmacia, Universidad de Sevilla, C/Profesor García González N° 2, 41012 Sevilla, España. Tel.: +34 954556618; fax: +34 954556085.
E-mail address: luciamartin@us.es (L. Martín-Banderas).

http://dx.doi.org/10.1016/j.ijpharm.2015.04.054
0378-5173/

2013a,b). However, the micrometer size of the Δ^9-THC particulate formulation (≈20–50 μm) is expected to limit the clinical outcome (Decuzzi et al., 2009).

As an alternative, poly(D,L-lactide-*co*-glycolide) nanoparticles (PLGA NPs) have been investigated (Martín-Banderas et al., 2014). This PLGA-based formulation was also used as nanocarrier for synthetic cannabinoid receptor agonist 13 (CB13) molecules (Durán-Lobato et al., 2013; Martín-Banderas et al., 2012). However, a definitive *in vitro* and *in vivo* proof of concept of the possibilities of this (Δ^9-THC)-loaded nanoparticulate formulation is needed.

Therefore, this work is devoted to the development of PLGA-based nanocarriers as delivery systems for Δ^9-THC. Concretely, PLGA NPs, PLGA NPs surface coated with poly(ethylene glycol) (PEGylated PLGA NPs), PLGA NPs embedded within a chitosan (CS) shell (chitosan-coated PLGA NPs), and PEGylated chitosan-coated PLGA NPs were investigated. Vitamin E molecules were incorporated to the formulations to enhance the stability of Δ^9-THC against oxidation. Geometry and surface electrical charge measurements, blood compatibility and protein adsorption characterizations, and the *in vitro* evaluation of the Δ^9-THC loading and release capabilities revealed that the PEGylated PLGA nanosystem was the more adequate formulation for the parenteral administration of Δ^9-THC (see below). Finally, the *in vitro* anticancer activities of (Δ^9-THC)-loaded PEGylated PLGA NPs were evaluated in murine LL2 and human A-549 lung cancer cell lines. The human embryo lung fibroblastic MRC-5 cell line was used as control. Regarding the *in vivo* investigation of the antitumor potential of (Δ^9-THC)-loaded PEGylated PLGA NPs, LL2 lung tumor-bearing immunocompetent C57BL/6 mice was used to that aim.

2. Materials and methods

2.1. Materials

Δ^9-THC was provided by THC Pharm (Frankfurt am Main, Germany). PLGA (Resomer® RG 502, PLGA 50:50, molecular weight: 12,000 Da, inherent viscosity: 0.24 dL/g) was obtained from Boehringer-Ingelheim (Ingelheim, Germany). Low molecular weight chitosan, Span® 60, Tween® 80, Pluronic® F-68, ethylenediaminetetraacetic acid (EDTA), trypsin, sodium citrate, 3-(4,5-dimethylthiazol-2-yl)-2,5-diphenyltetrazolium bromide (MTT), Triton® X-100, ammonium oxalate, sodium dodecyl sulphate (SDS), monoclonal antibody specific for human C3a desArg peroxidase-conjugated rabbit anti-C3a and fluorochrome nile red were purchased from Sigma–Aldrich (St Louis, MO, USA). Glycerol was obtained from Acofarma Distribución S.A. (Barcelona, Spain). Vitamin E was a generously gift from ChemTrade GmbH (Burgbernheim, Germany). Threalose was obtained from VWR International Eurolab S.L. (Barcelona, Spain).

PEG (molecular weight: 20 kDa) was obtained from Serva Feinbiochemica GmbH & Co. (Heidelberg, Germany). PEG molecular weights and PEG chain lengths may have a significant influence on the prevention of the surface adsorption of plasma proteins onto NPs (and thus, plasma clearance) (Gref et al., 2000). It is accepted that increasing PEG chain lengths (thus PEG molecular weights) minimizes protein adsorption onto PEGylated NPs (preventing plasma clearance). Hence, this is the reason why PEG with a molecular weight of 20 kDa was used, instead of other PEGs, *e.g.*, from 2000 to 5000 Da.

All other chemicals were purchased from Panreac Química (Barcelona, Spain). Deionized and filtered water was used in all the experiments (Milli-Q Academic, Millipore, Molsheim, France). The release medium (phosphate buffered saline, PBS, pH 7.4) was obtained from Biochemica AppliChem (Darmstadt, Germany).

Human embryo lung fibroblastic MRC-5 and human lung adenocarcinoma A-549 cell lines were obtained from the European Collection of Cell Cultures (ECACC). The murine lung carcinoma LL2 cell line was obtained from the Scientific Instrumentation Centre of the University of Granada (Granada, Spain). The cell lines were maintained in Dulbecco's modified Eagle's medium (DMEM high glucose, with L-glutamine, phenol red and without pyruvate) with penicillin–streptomycin, which were obtained from PAA Laboratories (Pasching, Austria), and supplemented with Fetal Bovine Serum (FBS, Stemcell Technologies Inc.).

2.2. Synthesis and characterization of the PLGA-based nanoformulations

PLGA-based NPs were prepared by following the nanoprecipitation method (Fessi et al., 1989; Martín-Banderas et al., 2014). Briefly, a weighted amount of PLGA was dissolved with Span® 60 in acetone to obtain a 1.5% (w/v) concentration. Then, 5 mL of such solution were added drop-wise to 15 mL of a Pluronic® F-68 aqueous solution (0.5%, w/v) under magnetic stirring. Acetone was evaporated at room temperature during 4 h, to obtain an aqueous dispersion which was finally centrifuged to collect the NPs (10,000 rpm, 15 min, 4 °C; Eppendorf 504R, Eppendorf AG, Hamburgo, Germany). After washing twice, the NPs were re-suspended in a 5% (w/v) threalose solution (used as cryoprotectant) and freeze-dried (frozen in liquid nitrogen and lyophilized, −80.0 ± 0.5 °C, 0.057 mbar; Telstar Cryodos-50; Telstar Industrial S. L., Tarrasa, Spain) to obtain a fine whitish powder. All the formulations were prepared in triplicate.

Surface modification of the PLGA NPs with chitosan and/or PEG was done to improve the NP cellular uptake and to minimize the opsonization process that may take place in blood (Gref et al., 2000; Parveen and Sahoo, 2011). To that aim, chitosan or PEG was added to the NP aqueous dispersion upon evaporating acetone. Briefly, PLGA NPs were incubated overnight in a 0.25% (w/v) chitosan solution in 1% (v/v) acetic acid to obtain chitosan-coated PLGA NPs. PEGylation of the chitosan-coated PLGA NPs (or PLGA NPs) was accomplished by incubating the particles in a 4.5% (w/v) PEG solution during 3 h. Finally, the PEGylated chitosan-coated PLGA NPs (or PEGylated PLGA NPs) were collected by centrifugation (10,000 rpm, 15 min, 4 °C).

To sum up, 4 nanoformulations were synthesized, *i.e.*, PLGA NPs, chitosan-coated PLGA NPs (CS–PLGA NPs), PEGylated PLGA NPs (PEG–PLGA NPs), and PEGylated chitosan-coated PLGA NPs (PEG–CS–PLGA NPs).

On the basis of the best drug incorporation conditions defined previously (Martín-Banderas et al., 2014), Δ^9-THC-PLGA was loaded to the nanoparticulate systems. Briefly, the procedure started by adding 2.25 mL of a Δ^9-THC solution in acetone (1 mg/mL) to the PLGA organic solution before starting the nanoprecipitation procedure. The drug/polymer concentration in this solution was 5% (w/w). In addition, the antioxidant additive vitamin E was incorporated to that organic solution to prevent Δ^9-THC oxidation (vitamin/polymer concentration: 5%, w/w).

Mean particle size was determined at 25.0 ± 0.5 °C by a laser scattering technique based on the Mie theory (Partica LA-950V2, Horiba Ltd., Kyoto, Japan). Measurements of aqueous dispersions of the PLGA-based NPs (0.1%, w/v) were carried out under continuous magnetic agitation. To confirm the results transmission electron microscopy (TEM) characterizations were also done (CM-10 transmission electron microscope; Philips Electronics, Amsterdam, Holland) to particle samples prepared by drying the dispersions at room temperature overnight in a convection oven. Finally, the surface electrical charge of the NPs was determined in triplicate by zeta potential (ζ, mV) measurements (Zetamaster 3000, Malvern Instruments Ltd., Malvern, UK) at room temperature.

2.3. Drug loading and in vitro drug release determinations

Δ^9-THC loading to (and release from) the PLGA-based NPs was determined by a reverse phase-high performance liquid chromatography (RP-HPLC) method which was previously validated to demonstrate its precision, accuracy, and linearity. The RP-HPLC analysis was done with a Hitachi LaChrom® (D-7000) Series HPLC system equipped with a L-7200 automatic injector, a D-7000 interphase, a L-7100 quaternary pump, and a DAD UV–vis L-7455 detector. A Waters column (3 μm, 4.6 × 100 mm, Milford, MA, USA) maintained at 25.0 ± 0.1 °C (L-2350 column oven, Elite LaChrom®) was used in this analysis. Data collection and calculation were carried out with a HSM D-7000 LaChrom® software (Merck-Hitachi, Darmstadt, Germany).

Briefly, 5 mL of acetone was added to 5 mg of lyophilized NPs (accurately weighted with a high-precision analytical balance, d = 0.01 mg, model CP 225D; Sartorius AG, Göttingen, Germany). The mixture was mechanically stirred to dissolve the particles in acetone, which was finally evaporated (Büchi R/210 Rotary Evaporator, BüchiLabortechnik AG, Flawil, Switzerland). Then, 1 mL of methanol was added and mechanical stirring was continued during 5 min. The drug solution was filtered (0.22 μm syringe filter, Millex® GV, Millipore, Barcelona, Spain) and injected into the HPLC system for Δ^9-THC detection. Drug incorporation to the NPs was indicated as entrapment efficiency (EE, %) and drug loading (DL, %), as follows:

$$EE(\%) = \left(\frac{\text{amount of}\Delta^9 - \text{THC loaded (mg)}}{\text{initial amount of}\Delta^9 - \text{THC loaded (mg)}}\right) \times 100 \quad (1)$$

$$DL(\%) = \left(\frac{\text{amount of}\Delta^9 - \text{THC (mg)}}{\text{amount of NPs obtained}}\right) \times 100 \quad (2)$$

In vitro drug release studies were carried out by incorporating 4 mg of NPs to 15 mL of phosphate buffered saline (PBS) (pH 7.4) containing 0.1% (w/v) of Tween® 80 to keep the sink conditions (Hombreiro-Perez et al., 2003). The experiments were done in triplicate at 37 °C and under mechanical stirring (100 rpm, Unitronic OR, Selecta S.A., Barcelona, Spain). Aliquots (500 μL) were withdrawn at predetermined time intervals, centrifuged (10,000 rpm, 5 min; Eppendorf 504R, Eppendorf AG, Hamburgo, Germany), and filtered (0.22 μm syringe filter, Millex® GV, Millipore, Barcelona, Spain). Finally, 20 μL of these aliquots was injected into the HPLC apparatus to evaluate the Δ^9-THC content. To that aim, it was used a calibration curve constructed over the range 20–100 μg/mL (r^2 = 0.9990, limit of detection: 30 μg/mL, limit of quantification: 40 μg/mL).

2.4. Protein adsorption and blood compatibility studies

Regarding the protein adsorption tests, NPs were incubated in 1 mL of a 400 μg/mL bovine serum albumin (BSA) aqueous solution. Then, the dispersion was mechanically stirred with a magnetic stirrer during 2 h at 37 °C (Thiele et al., 2003; Parveen and Sahoo, 2011), and the NPs were centrifuged (10,000 rpm, 4 °C, 20 min; Eppendorf 504R; Eppendorf AG, Hamburgo, Germany) to remove any unabsorbed protein. Finally, samples were diluted in PBS (1:20) and zeta potential measurements were accomplished.

The interaction of nanoparticulate formulations with blood components has been postulated as an indicator of toxicity (Dash et al., 2010; Bender et al., 2012; Lekshmi and Reddy, 2012). Blood was obtained from six healthy female adults (30–42 years old), and poured into flasks containing either EDTA (used in the haemolysis, and platelet activation experiments), or sodium citrate (used in the complement system activation, and plasma clotting time experiments). Following a clearly defined method (Dash et al., 2010), the NPs were kept in contact with blood aliquots to evaluate their effect on erythrocytes, coagulation, and complement system. An UV spectrophotometric technique was satisfactorily validated and verified for accuracy, precision, and linearity.

2.5. In vitro cytotoxic activity

The anticancer activities of the (Δ^9-THC)-containing formulations were evaluated by using the MTT proliferation assay which measures the mitochondrial dehydrogenase activity (Vihola et al., 2005; Gustafsson et al., 2009). To that aim, murine LL2 and human A-549 lung cancer cell lines were used. The human embryo lung fibroblastic MRC-5 cell line was employed as control. The formulations involving the drug, *i.e.*, free Δ^9-THC, (Δ^9-THC)-loaded PLGA NPs, (Δ^9-THC)-loaded PEGylated PLGA NPs, and (Δ^9-THC)-loaded PEGylated chitosan-coated PLGA NPs, that were kept in contact with cells ranged from 0.1 to 50 μM equivalent drug concentration. In addition, NP concentration in these nanoformulations (further including drug-unloaded PLGA NPs) was in the same range of concentrations (0.06–0.32 mg/mL).A total number of cells/well from 2.7×10^3 to 4.5×10^3 cells/well were cultured in 96-well plate (Nunclon®, Thermo Fisher Scientific, Waltham, MA, USA) during 24 h at 37 °C. Then, the formulations were added to the cell culture. After 72 h of incubation, the medium was removed, 125 μL MTT (1 mg/mL in medium) was incorporated and the plates were incubated during 4 h at 37 °C. Next, 80 μL of 20% SDS in 0.02 M HCl was added and incubated during 10 h at 37 °C. The optical density of each well was measured at 540 nm (Synergy HT multiwell plate spectrophotometer reader, BioTek Instruments Inc., Winooski, VT, USA) to quantify cell viability. Cell survival (%) was calculated as percentage of viability compared to the control (non-treated cells).

2.6. In vivo anticancer studies

These studies were approved by the Ethics Committee of the University of Granada and performed according to its guidelines. A number of 40 immunocompetent female C57BL/6 mice (body weight ≈25 g, Charles River, Barcelona, Spain) were used. They were maintained at 22 ± 1 °C and 40–70% of relative humidity in a laminar airflow cabinet with a 12 h light/dark cycle, and under specific pathogen-free conditions. All mice were subcutaneously injected in the right hind flank with 5×10^5 LL2 cells dispersed in 200 μL of PBS. When tumors were palpable, mice were randomly distributed into 4 experimental groups (n = 10) and treated every 3 days with: control (non-treated mice), free Δ^9-THC, PEGylated PLGA NPs, and Δ^9-THC-loaded PEGylated PLGA NPs. This nanoparticulate system was selected for this study given its promising *in vitro* antitumor effect (see Figs. 4 and 5). The treatment consisted in a peritumoral injection during 21 days of the formulations (Δ^9-THC equivalent doses: 5 mg/Kg of body mass). At the moment of treatment administration, mice were weighted, the tumor size was measured, and the death of mice was recorded. Tumor volume (V, mm^3) was measured by using a digital caliper as follows:

$$V = \frac{a \times b^2 \times \pi}{6} \quad (4)$$

where a is the longest diameter and b is the shortest diameter.

2.7. Statistical analysis

Data is presented as mean ± standard deviation. In the *in vitro* cell culture assays, Student's *t*-test and one-way analysis of variance (ANOVA) were used to define the significance between two groups and among more than two groups, respectively (software SPSS version 15, SPSS IBM Statistics, Chicago, USA). Regarding the *in vivo* antitumor activity results, statistical analysis was performed using the Student's *t*-test (software SPSS version 15, SPSS IBM Statistics, Chicago, USA). The probability of mice survival (cumulative survival curves) was determined by the Kaplan Meier method, and the log-rank test was used to compare the fraction of surviving mice between groups ($\alpha = 0.05$). Data with $p < 0.05$ and $p < 0.001$ were considered as significant and very significant, respectively.

3. Results and discussion

3.1. Particle geometry and surface electrical charge

Mean particle size of PLGA NPs is increased from ≈300 nm to ≈600 nm or ≈750 nm when a polymeric coating is incorporated onto their surface, *i.e.*, PEG or chitosan, respectively (Table 1). It has been attributed such kind of increase in size to polymer deposition onto the NP surface in the form of multi-layers (Nafee et al., 2009; Parveen and Sahoo, 2011). In all cases the coefficient of variation is in the range of ≈15%, this indicating that the particle distributions were almost homogeneous. Taking into consideration particle sizes corresponding to the same nanoformulations prepared without using vitamin E (Martín-Banderas et al., 2014), it can be assumed that this additive does not seem to affect particle dimensions. Surface modification by using chitosan and/or PEG is expected to promote cellular uptake while keeping to a minimum NP opsonization (Gref et al., 2000; Parveen and Sahoo, 2011; Martín-Banderas et al., 2014). Finally, all the nanoformulations were characterized by a spherical shape.

In addition, PLGA NPs surface coated by chitosan and/or PEG were characterized by a core/shell structure that can be easily visualized by TEM (see Fig. 1 as an illustrative example). These results along with the previously reported FTIR data (Martín-Banderas et al., 2014) confirmed the core/shell structure of these nanoparticulate systems.

Regarding the surface electrical charge of the PLGA NPs, characteristic ζ negative values for pure PLGA NPs, turns into positive or almost neutral upon surface coating with chitosan or PEG, respectively (Table 1). The positive ζ values defined for the chitosan-coated PLGA NPs may come from the polycationic nature of chitosan (primary amino groups). On the contrary, the ζ values close to neutrality in the case of PEGylated NPs may be due to the displacement of the diffuse ionic layer to a greater distance from the particles by the PEG chains (Patel et al., 2012).

Table 1
Mean diameter (D_{mean}, nm) and zeta potential (ζ, mV) values of the PLGA-based nanoparticulate formulations loaded with Δ^9-THC (drug concentration: 5%, w/w) ($n = 12$) (S.D.: standard deviation).

Formulation	$D_{mean} \pm$ S.D. (nm)	$\zeta \pm$ S.D. (mV)
PLGA	290.10 ± 60.30	−34.78 ± 5.98
PEG–PLGA	587.90 ± 98.01	0.46 ± 0.06
CS–PLGA	746.89 ± 100.76	78.21 ± 7.65
PEG–CS–PLGA	789.67 ± 95.34	5.34 ± 0.98

3.2. Drug vehiculization

Results obtained from Δ^9-THC incorporation experiments to PLGA NPs are collected in Table 2. Similar drug loading values were obtained in PLGA NPs and in PLGA NPs surface modified with chitosan and/or PEG, thus the polymeric surface coating to the PLGA NPs did not positively influence the drug loading efficiencies. In fact, EE (%) and DL (%) values were always in the range of ≈95% to ≈97% and ≈4.8% to ≈4.9%, respectively. In any case, and independently of the preparation conditions, Δ^9-THC was reproducibly and efficiently loaded to the NPs probably thanks to the apolar character of Δ^9-THC which avoids its migration into the aqueous phase during NP synthesis (Barichello et al., 1999). Furthermore, the use of vitamin E in NP preparation to some extent influenced Δ^9-THC loading. In fact, Δ^9-THC entrapment efficiencies were slightly reduced when vitamin E was not used in NP synthesis (Martín-Banderas et al., 2014). This is because of the surfactant nature of the additive which gets to improve the stability and the quality of the organic/aqueous interface during NP synthesis (Duhem et al., 2014). Vitamin E mixed with the nonionic surfactants used in the synthesis of the nanoformulations provides an increase in stability of the nanoparticles wall (Li et al., 2011).

Regarding Δ^9-THC release from the nanoparticulate systems, a biphasic profile consisting of a rapid phase followed by a slow release phase was observed (Fig. 2). Concretely, up to ≈20% of the Δ^9-THC molecules entrapped within the PLGA NPs (△, black line), ≈10% of the Δ^9-THC molecules entrapped within the chitosan-coated PLGA NPs (□, dashed line), ≈60% of the Δ^9-THC molecules entrapped within the PEGylated PLGA NPs (▲, black line), and ≈20% of the Δ^9-THC molecules entrapped within the PEGylated chitosan-coated PLGA NPs (◇, dashed line), were released in ≈1 day, ≈4 days, ≈3 days, and ≈1 day, respectively; the remaining drug being released in a sustained manner over a period of ≈9 days, ≈6 days, ≈7 days, and ≈9 days, respectively. This is the

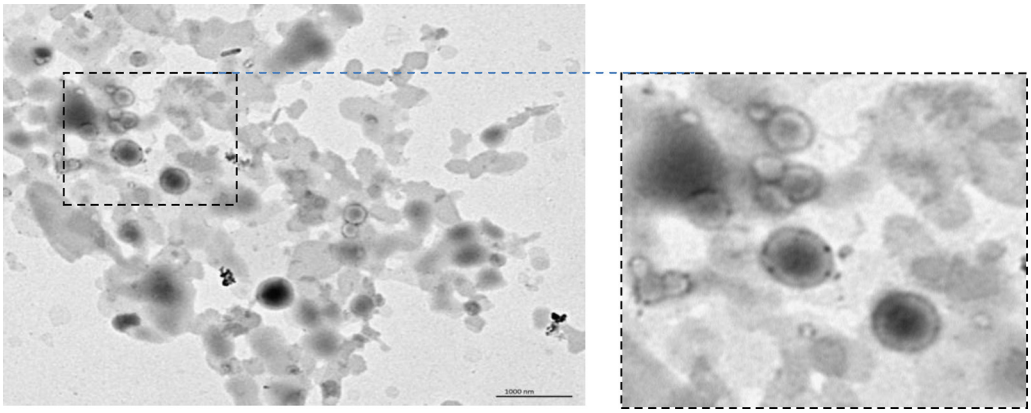

Fig. 1. Transmission electron microphotographs of chitosan-coated PLGA NPs. Bar length: 1000 nm.

Table 2
Δ^9-THC entrapment efficiency (EE, %) and Δ^9-THC loading (DL, %) values of the PLGA-based nanoparticulate formulations ($n = 12$).

Nanoformulation	EE (%)	DL (%)
PLGA	95.5 ± 0.2	4.8 ± 0.1
PEGylated PLGA	97.4 ± 0.3	4.9 ± 0.1
Chitosan-coated PLGA	96.3 ± 0.6	4.8 ± 0.2
PEGylated chitosan-coated PLGA	94.9 ± 0.8	4.8 ± 0.1

consequence of the well-known drug diffusion process characteristic of hydrophobic and semi-crystalline PLGA nanomatrices (Fu et al., 2000; Chan et al., 2009; Kumari et al., 2010; Patel et al., 2012). Chitosan surface coating of the PLGA NPs prolonged Δ^9-THC release probably because Δ^9-THC molecules must diffuse through a core/shell matrix greater than the pure PLGA matrices (Table 1). On the contrary, PEGylation accelerated Δ^9-THC release from PLGA NPs and chitosan-coated PLGA NPs presumably due to the polar nature of PEG chains which facilitates the contact of the NP matrices with water molecules (and thus PLGA hydrolysis and drug diffusion) (Martín-Banderas et al., 2014).

As previously highlighted, vitamin E was incorporated to the nanoformulations to prevent Δ^9-THC degradation, process that may occur under the acidic environment resulting from PLGA degradation (Fu et al., 2000; Traber and Atkinson, 2007; Astete et al., 2011; Klose et al., 2011; Hernán Pérez de la Ossa et al., 2012; Tran et al., 2012). In order to define the protective effect of vitamin E to the Δ^9-THC molecules incorporated into the NPs, the remaining amount of drug molecules (into the NPs prepared with or without the antioxidant agent) after a 144 h of releasing process (under the conditions detailed in Section 2.3) was extracted and measured by HPLC. Compared to the antioxidant-free nanoformulations, an enhancement of ≈ 67% in the stability of Δ^9-THC was measured which led to a 10-day release profile when vitamin E was incorporated to the NPs. Thus, the use of vitamin E can (protect and) prolong drug release from the PLGA-based nanoparticulate systems (Barcia et al., 2005; Hernán Pérez de la Ossa et al., 2013a; Herrero-Vanrell et al., 2014). On the opposite, a 6-day release profile was characteristic of the vitamin E-free nanoformulations (Martín-Banderas et al., 2014).

3.3. Protein adsorption and blood compatibility

Numerous investigations have defined the protective effect of hydrophilic polymer chains (*i.e.*, PEG) located onto NP surface against opsonization and plasma clearance. In fact, PEGylation has been suggested to be necessary to assure NP accumulation into the targeted cell/tissue (Gref et al., 2000; Decuzzi et al., 2009; Reddy et al., 2012; Sempf et al., 2013). In our investigation, BSA was used as a model protein to evaluate NP interaction with blood proteins (Thiele et al., 2003; Parveen and Sahoo, 2011).

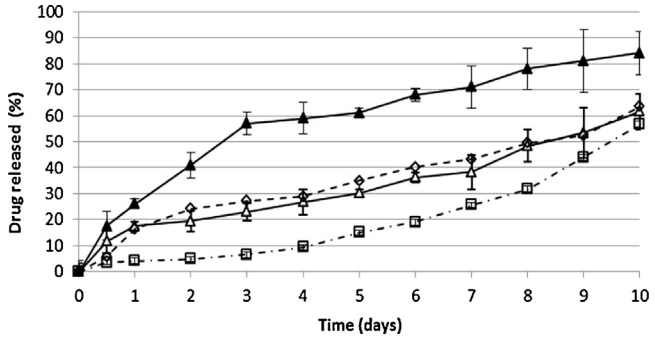

Fig. 2. *In vitro* Δ^9-THC release (%) from PLGA (△, black line), chitosan-coated PLGA (□, dashed line), PEGylated PLGA (▲, black line) and PEGylated chitosan-coated PLGA (◇, dashed line) NPs as a function of the time (days) ($n = 3$).

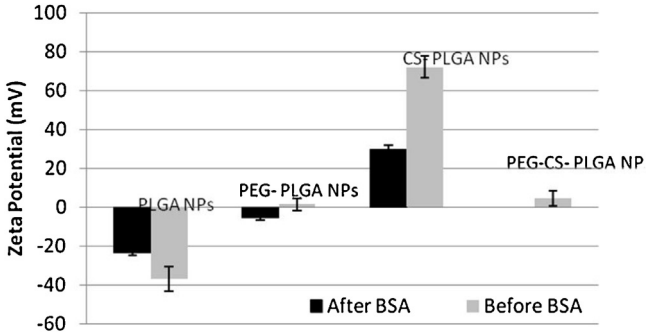

Fig. 3. Zeta potential (mV) values of PLGA NPs, PEGylated PLGA (PEG-PLGA) NPs, chitosan-coated PLGA (CS-PLGA) NPs, and PEGylated chitosan-coated PLGA (PEG–CS–PLGA) NPs before and after contacting with BSA.

Fig. 3 illustrates how the ζ values are significantly reduced when non-PEGylated NPs are in contact with BSA molecules, the consequence of an intense protein adsorption. On the opposite, the surface electrical charge of PEGylated NPs is not significantly affected. This information may be advantageously used to estimate how PEGylated NPs may evade the recognition by the RES in their way to the targeted site of action, compared to non-PEGylated NPs (Jokerst et al., 2011; Sempf et al., 2013). According to this information, non-PEGylated chitosan-coated PLGA NPs were discarded in the *in vitro* anticancer activity experiments.

Results collected in Table 3 clearly define the adequate *in vivo* safety margin of all of the PLGA-based nanoformulations. These nanosystems can be considered haemocompatible for drug delivery applications. In fact, the particles are expected to exhibit a negligible effect on haemolysis, not affecting sP-selectin release levels (from platelet activation quantification), complement system activation, and plasma clotting times. Similar results have been reported for other nanoparticulate systems with significant *in vivo* safety margin (Dash et al., 2010; Arias et al., 2011; Martín-Banderas et al., 2012; Pérez-Artacho et al., 2012).

3.4. In vitro anticancer activity

The cytotoxic activity of the (Δ^9-THC)-containing formulations was firstly investigated *in vitro* in human embryo lung fibroblastic MRC-5 and human lung adenocarcinoma A-549 cell lines (Fig. 4). With respect to the free drug, it was found to be more cytotoxic to A-549 cells than to MRC-5 cells. Such significant difference suggests a certain selectivity of action for cancer cells which may be justified if it is taken into account that the CB1 and CB2 cannabinoids receptors are overexpressed in lung cancer cells (Preet et al. 2008; Takeda et al. 2008; Moreno et al. 2014). These findings were also observed in the Δ^9-THC-loaded PLGA-based nanosystems (Fig. 4a and b) while drug unloaded PLGA NPs did not develop any cytotoxic activity (data not shown).

Viability of MRC-5 cells was significantly affected by the type of nanoparticulate system ($F = 25.270$, $p < 0.05$, $n = 16$), being the (Δ^9-THC)-loaded PEGylated PLGA NP formulation the one producing the greatest anticancer effect [*post hoc* Student–Newman–Keuls (SNK)] (Fig. 4a). Cell proliferation was observed when using (Δ^9-THC)-loaded PEGylated chitosan-coated PLGA NPs, and with (Δ^9-THC)-loaded PLGA NPs, probably a consequence of the very slow Δ^9-THC release kinetics characteristic of these nanoformulations (Fig. 2) that determine a smaller effective drug concentration in contact with the cells (Hernán Pérez de la Ossa et al., 2012, 2013b). In any case, the limited expression of CB1 and CB2 cannabinoids receptors in MRC-5 cells may be responsible for the negligible

Table 3
Blood compatibility of the nanoparticulate formulations in terms of haemolysis (%), platelet activation [soluble P-selectin (sP-selectin) release, ng/mL], complement activation (C3a desArg ng/mL) and plasma recalcification time ($T_{1/2max}$, min).

Formulation	Haemolysis (%)	sP-selectin release (ng/mL)	C3a desArg (ng/mL)	$T_{1/2}$max (min)
PLGA NPs	2.1 ± 0.2	96 ± 9	293 ± 7	10.5 ± 0.7
(Δ^9-THC)-loaded PLGA NPs	1.9 ± 0.4	103 ± 7	289 ± 8	11.1 ± 0.5
PEGylated PLGA NPs	2.2 ± 0.6	104 ± 5	291 ± 5	12.1 ± 0.8
(Δ^9-THC)-loaded PEGylated PLGA NPs	1.8 ± 0.8	101 ± 8	296 ± 8	11.6 ± 1.2
PEGylated chitosan-coated PLGA NPs	2.3 ± 0.6	106 ± 4	294 ± 7	12.4 ± 0.9
(Δ^9-THC)-loaded PEGylated chitosan-coated PLGA NPs	2.4 ± 0.3	98 ± 9	288 ± 9	11.7 ± 1.3
Control (PBS solution)	0	97 ± 13	284 ± 12	12.3 ± 1.1

activity of Δ^9-THC in this cell line, even in the form of free molecules. In fact, only at the greater equivalent drug concentration (50 μM), the PEGylated PLGA nanoformulation exhibited some negative effect on MRC-5 viability.

Compared to MRC-5 cells (Fig. 4a), the *in vitro* anticancer activity of Δ^9-THC-loaded PLGA-based particles against A-549 cells was clear and positively affected by the Δ^9-THC equivalent concentration (Fig. 4b) ($F = 35.676$, $p < 0.05$, $n = 16$), being the cytotoxic effect of (Δ^9-THC)-loaded PEGylated PLGA NPs 1.4-fold greater than free drug. Concretely, the inhibitory concentration 50 (IC_{50}) values of free Δ^9-THC and (Δ^9-THC)-loaded PEGylated PLGA NPs in MRC-5 cells were found to be 99.2 ± 41.4 μM and 76.2 ± 20.6 μM, respectively (meaning a 1.63-fold decrease); and 60.8 ± 23.6 μM and 42.3 ± 29.3 μM, respectively in A-549 cells. These IC_{50} values were mathematically determined using the point to point method in *Excel* or by linear extrapolation from the corresponding concentration-response curve when IC_{50} values were not within the range of tested concentrations. Finally, viability of A-549 cells was significantly influenced by the type of drug-loaded nanostructure ($F = 13.368$, $p < 0.05$, $n = 12$). In this case, the *post hoc* SNK differentiated the effect of the (Δ^9-THC)-loaded nanoformulations: PEGylated PLGA > PEGylated chitosan-coated PLGA > PLGA.

The greater activity of Δ^9-THC molecules against A-549 cells when loaded to PEGylated PLGA NPs is probably the result of the sum of the differences on cannabinoids receptors expression between cell lines and of a protective role against degradation displayed by the nanoparticulate matrix on the drug molecules. In addition, vitamin E was incorporated to the nanoformulation to prevent Δ^9-THC degradation (see Section 3.2), *i.e.*, by oxidation, temperature, and/or light. Thus, drug molecules loaded to the NPs (also containing vitamin E) may be protected from unfavorable conditions determining their degradation. This may be the reason why: (i) a greater antitumor effect was found in the nanoparticulate formulations compared to the free drug; and (ii) even at the greater drug concentrations (50 μM), the cytotoxic activity of the free Δ^9-THC could be considered to be very poor (almost negligible) in contrast to Δ^9-THC-loaded NPs.

Same hypothesis should be used to explain both the null cytotoxic effect of Δ^9-THC molecules in murine lung adenocarcinoma LL2 cells (the cell line used in the *in vivo* studies, see Sections 2.6 and 3.5), and the clearly greater cytotoxic activity of (Δ^9-THC)-loaded PEGylated PLGA NPs in LL2 cells compared to free Δ^9-THC. Again, the PEGylated nanoformulation reported a greater reduction in LL2 cell viability in comparison to free Δ^9-THC (significant differences were appreciated at concentrations ≥10 μM, $p < 0.05$) (Fig. 5). Drug unloaded PEGylated PLGA NPs did not develop any cytotoxic activity (data not shown).

3.5. In vivo tumor growth inhibition and survival analysis

The anticancer activity of free Δ^9-THC, PEGylated PLGA NPs, and Δ^9-THC-loaded PEGylated PLGA NPs was investigated in LL2 lung tumor-bearing immunocompetent C57BL/6 mice (Fig. 6). No statistically significant differences in terms of antitumor effect were observed during the first 4 weeks of treatment. Compared to the control group and the free Δ^9-THC, Δ^9-THC-loaded PEGylated PLGA NPs reported a 2.2-fold reduction in tumor volume on day 32, which was finally measured to be a 1.5-fold reduction on day 41 (end of the experiment). In any case, no statistically significant differences were defined between the groups in terms of tumor volume reduction (Fig. 6a) and cumulative survival (Fig. 6c). In

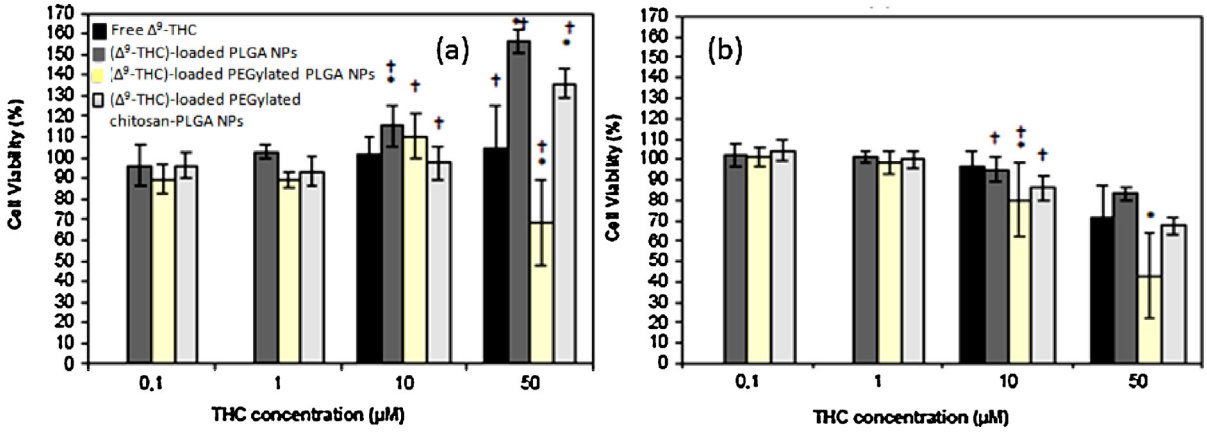

Fig. 4. Cell viability (%) values of (a) MRC-5 and (b) A-549 cells upon contacting with free Δ^9-THC, (Δ^9-THC)-loaded PLGA NPs, (Δ^9-THC)-loaded PEGylated PLGA NPs, and (Δ^9-THC)-loaded PEGylated chitosan-coated PLGA NPs. Drug equivalent dose in μM, $n = 4$. An asterisk represents a statistically significant difference between free-Δ^9-THC and Δ^9-THC-loaded PLGA nanoparticles at the same concentration in the same cell line. A dagger represents a statistically significant difference between free-Δ^9-THC and Δ^9-THC-loaded PLGA nanoparticles at the same concentration between the two cell lines studied (ANOVA test).

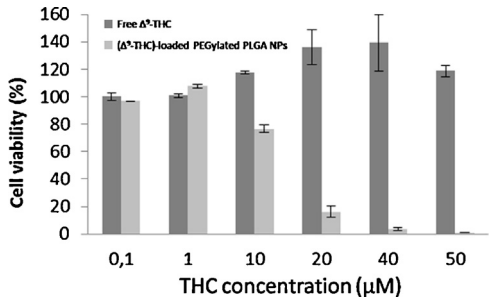

Fig. 5. Cell viability (%) values of LL2 cells upon contacting with free Δ^9-THC and (Δ^9-THC)-loaded PEGylated PLGA NPs. Drug equivalent dose in μM, $n = 4$.

addition, no disparities were detected in the tumor necropsies of the animals included in the 4 study groups. Finally, the similarities found between the control group and the groups of mice under treatment in terms of evolution of body weight (along with the blood compatibility investigation) suggested the adequate *in vivo* safety margin of the formulations.

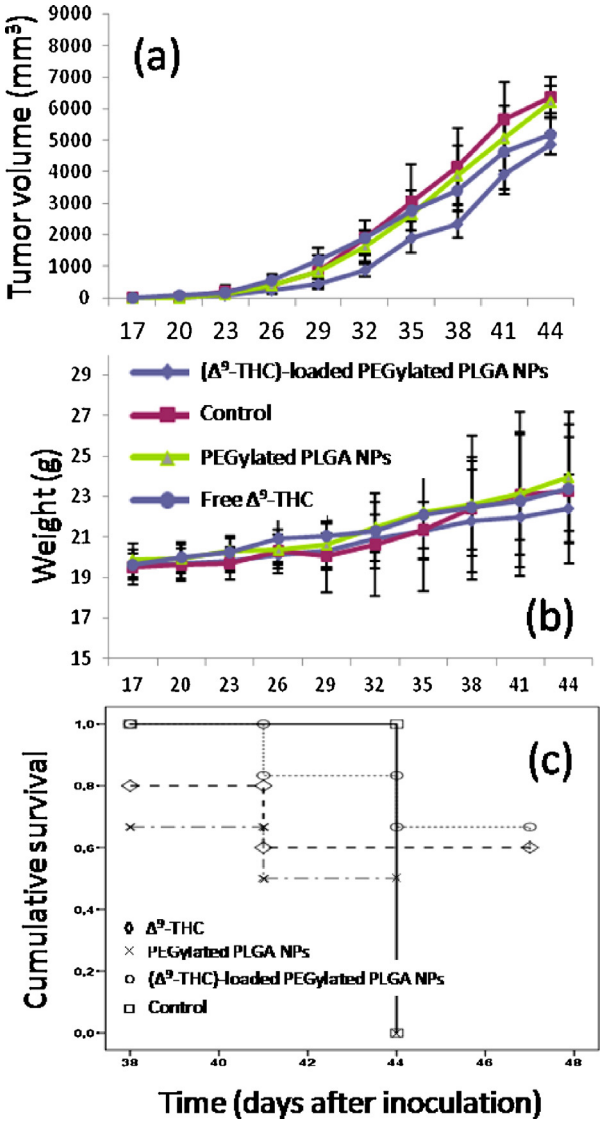

Fig. 6. Evolution of (a) tumor volume (mm^3) and (b) weight (g), and (c) cumulative survival in LL2 lung tumor-bearing immunocompetent C57BL/6 mice treated with free Δ^9-THC, PEGylated PLGA NPs, and (Δ^9-THC)-loaded PEGylated PLGA NPs ($n = 10$). Control group: no treatment.

4. Conclusions

A reproducible nanoprecipitation technique has been proposed to prepare PLGA-based nanoformulations loaded with Δ^9-THC. The nanosystems are characterized by an adequate *in vivo* safety margin, high drug loading efficiencies, and sustained drug release properties. Surface modification with PEG chains can improve the Δ^9-THC vehiculization capabilities and reduce protein adsorption (and thus probably the *in vivo* opsonization processes). Vitamin E has been advantageously included in the nanoformulations to protect the drug from degradation. *In vitro* anticancer studies highlighted the promising activity of (Δ^9-THC)-loaded PEGylated PLGA NPs against murine lung adenocarcinoma LL2 and human lung adenocarcinoma A-549 cell lines. Further *in vivo* studies are encouraged to clarify the potential application of the nanoformulation in lung cancer chemotherapy. In this line, supplementary surface modifications, *i.e.*, decoration of the particle surface with ligands specific to receptors overexpressed onto the cancer cell membrane, may optimize the selectivity of these (Δ^9-THC)-loaded nanoparticulate systems toward tumor cells.

Acknowledgements

The research leading to these results has received funding from projects P09-CTS-5029 (Consejería de Innovación, Junta de Andalucía, Spain), PE-2012-FQM-694 (Consejería de Innovación, Junta de Andalucía, Spain), and FIS 11/02571 (Instituto de Salud Carlos III, Spain). L.M.-B. is especially grateful for the financial support from Junta de Andalucía (España). We also thank Microscopy and Biology Services of CITIUS (University of Seville) for technical assistance.

References

Arias, J.L., López-Viota, M., Sáez-Fernández, E., Ruiz, M.A., Delgado, A.V., 2011. Engineering of an antitumor (core/shell) magnetic nanoformulation based on the chemotherapy agent ftorafur. Colloids Surf. A Physicochem. Eng. Aspects 384, 157–163.

Astete, C.E., Dolliver, D., Whaley, M., Khachatryan, L., Sabliov, C.M., 2011. Antioxidant poly(lactic-*co*-glycolic) acid nanoparticles made with α-tocopherol-ascorbic acid surfactant. ACS Nano 5, 9313–9325.

Aviello, G., Romano, B., Borrelli, F., Capasso, R., Gallo, L., Piscitelli, F., Di Marzo, V., Izzo, A.A., 2012. Chemopreventive effect of the non-psychotropic phytocannabinoid cannabidiol on experimental colon cancer. J. Mol. Med. (Berl.) 90, 925–934.

Barcia, E., Herradón, C., Herrero-Vanrell, R., 2005. Biodegradable additives modulate ganciclovir release rate from PLGA microspheres destined to intraocular administration. Lett. Drug Des. Discov. 2, 148–149.

Barichello, J.M., Morishita, M., Takayama, K., Nagai, T., 1999. Encapsulation of hydrophilic and lipophilic drugs in PLGA nanoparticles by the nanoprecipitation method. Drug Dev. Ind. Pharm. 25, 471–476.

Bender, E.A., Adorne, M.D., Colomé, L.M., Abdalla, D.S., Guterres, S.S., Pohlmann, A.R., 2012. Hemocompatibility of poly(ε-caprolactone) lipid-core nanocapsules stabilized with polysorbate 80-lecithin and uncoated or coated with chitosan. Int. J. Pharm. 426, 271–279.

Bifulco, M., Laezza, C., Pisanti, S., Gazzerro, P., 2006. Cannabinoids and cancer: pros and cons of an antitumour strategy. Br. J. Pharmacol. 148, 123–135.

Blázquez, C., González-Feria, L., Alvarez, L., Haro, A., Casanova, M.L., Guzmán, M., 2004. Cannabinoids inhibit the vascular endothelial growth factor pathway in gliomas. Cancer Res. 64, 5617–5623.

Brownjohn, P.W., Ashton, J.C., 2012. Cannabinoids and neuropathic pain. In: Cyprian Chukwunonye Udeagha (Ed.), Neuropathic Pain. InTech Open Science, Rijeka, Croatia, pp. 79–102.

Casanova, M.L., Blázquez, C., Martínez-Palacio, J., Villanueva, C., Fernández-Aceñero, M.J., Huffman, J.W., Jorcano, J.L., Guzmán, M., 2003. Inhibition of skin tumor growth and angiogenesis in vivo by activation of cannabinoid receptors. J. Clin. Invest. 111, 43–50.

Chan, J.M., Zhang, L., Yuet, K.P., Liao, G., Rhee, J.W., Langer, R., Farokhzad, O.C., 2009. PLGA-lecithin-PEG core–shell nanoparticles for controlled drug delivery. Biomaterials 30, 1627–1634.

Dash, B.C., Réthoré, G., Monaghan, M., Fitzgerald, K., Gallagher, W., Pandit, A., 2010. The influence of size and charge of chitosan/polyglutamic acid hollow spheres on cellular internalization, viability and blood compatibility. Biomaterials 31, 8188–8197.

Decuzzi, P., Pasqualini, R., Arap, W., Ferrari, M., 2009. Intravascular delivery of particulate systems: does geometry really matter? Pharm. Res. 26, 235–243.
Duhem, N., Danhier, F., Préat, V., 2014. Vitamin E-based nanomedicines for anti-cancer drug delivery. J. Controlled Release 182, 33–44.
Durán-Lobato, M., Muñoz-Rubio, I., Holgado, M.A., Álvarez-Fuentes, J., Fernández-Arévalo, M., Martín-Banderas, L., 2013. Enhanced cellular uptake and biodistribution of a synthetic cannabinoid loaded in surface-modified PLGA nanoparticles. J. Biomed. Nanotechnol. 10, 1068–1079.
Fessi, H., Puisieux, F., Devissaguet, J.P., Ammoury, N., Benita, S., 1989. Nanocapsule formation by interfacial polymer deposition following solvent displacement. Int. J. Pharm. 55, R1–R4.
Fu, K., Pack, D.W., Klibanov, A.M., Langer, R., 2000. Visual evidence of acidic environment within degrading poly(lactic-*co*-glycolic acid) (PLGA) microspheres. Pharm. Res. 17, 100–106.
Gref, R., Lück, M., Quellec, P., Marchand, M., Dellacherie, E., Harnisch, S., Blunk, T., Müller, R.H., 2000. Stealth corona-core nanoparticles surface modified by polyethylene glycol (PEG): influences of the corona (PEG chain length and surface density) and of the core composition on phagocytic uptake and plasma protein adsorption. Colloids Surf. B Biointerfaces 18, 301–313.
Gustafsson, S.B., Lindgren, T., Jonsson, M., Jacobsson, S., 2009. Cannabinoid receptor-independent cytotoxic effects of cannabinoids in human colorectal carcinoma cells: synergism with 5-fuorouracil. Cancer Chemother. Pharmacol. 63, 691–701.
Hernán Pérez de la Ossa, D., Ligresti, A., Gil-Alegre, M.E., Aberturas, M.R., Molpeceres, J., Di Marzo, V., Torres Suárez, A.I., 2012. Poly-ε-caprolactone microspheres as a drug delivery system for cannabinoid administration: development, characterization and in vitro evaluation of their antitumoral efficacy. J. Controlled Release 161, 927–932.
Hernán Pérez de la Ossa, D., Gil-Alegre, M.E., Ligresti, A., Aberturas, M.R., Molpeceres, J., Torres, A.I., Di Marzo, V., 2013a. Preparation and characterization of Δ^9-tetrahidrocannabinol-loaded-biodegradable polymeric microparticles and their antitumoral efficacy on cancer cell lines. J. Drug Target. 21, 710–718.
Hernán Pérez de la Ossa, D., Lorente, M., Gil-Alegre, M.E., Torres, S., García-Taboada, E., Aberturas, M.R., Molpeceres, J., Velasco, G., Torres-Suárez, A.I., 2013b. Local delivery of cannabinoid-loaded microparticles inhibits tumor growth in a murine xenograft model of glioblastoma multiforme. PLoS One 8, e54795.
Herrero-Vanrell, R., Bravo-Osuna, I., Andrés-Guerrero, V., Vicario-de-la-Torre, M., Molina-Martínez, I.T., 2014. The potential of using biodegradable microspheres in retinal diseases and other intraocular pathologies. Prog. Retin. Eye Res. 42, 27–43.
Hombreiro-Perez, M., Siepmann, J., Zinutti, C., Lamprecht, A., Ubrich, N., Hoffman, M., Bodmeier, R., Maincent, P., 2003. Non-degradable microparticles containing a hydrophilic and/or a lipophilic drug: preparation, characterization and drug release modelling. J. Controlled Release 88, 413–428.
Jokerst, J.V., Lobovkina, T., Zare, R.N., Gambhir, S.S., 2011. Nanoparticle PEGylation for imaging and therapy. Nanomedicine 6, 715–728.
Kumari, A., Yadav, S.K., Yadav, S.C., 2010. Biodegradable polymeric nanoparticles based drug delivery systems. Colloids Surf. B Biointerfaces 75, 1–18.
Lekshmi, U., Reddy, P., 2012. Preliminary toxicological report of metformin hydrochloride loaded polymeric nanoparticles. Toxicol. Int. 19, 267–272.
Li, X., Anton, N., Ta, T.M.C., Zhao, M., Messaddeq, N., Vandamme, T.F., 2011. Microencapsulation of nanoemulsions: novel Trojan particles for bioactive lipid molecule delivery. Int. J. Nanomed. 6, 1313–1325.
Machado-Rocha, F.C., dos Santos Junior, J.G., Stefano, S.C., da Silveira, D.X., 2014. Systematic review of the literature on clinical and experimental trials on the antitumor effects of cannabinoids in gliomas. J. Neurooncol. 116, 11–24.
Martín-Banderas, L., Álvarez-Fuentes, J., Durán-Lobato, M., Prados, J., Melguizo, C., Fernández-Arévalo, M., Holgado, M.A., 2012. Cannabinoid derivate-loaded PLGA nanocarriers for oral administration: formulation, characterization and cytotoxicity studies. Int. J. Nanomed. 7, 5793–5806.
Martín-Banderas, L., Muñoz-Rubio, I., Alvarez-Fuentes, J., Durán-Lobato, M., Arias, J. L., Holgado, M.A., Fernández-Arévalo, M., 2014. Engineering of Δ^9-tetrahydrocannabinol delivery systems based on surface modified-PLGA nanoplatforms. Colloids Surf. B Biointerfaces 123, 114–122.
McKallip, R.J., Lombard, C., Fisher, M., Martin, B.R., Ryu, S., Grant, S., Nagarkatti, P.S., Nagarkatti, M., 2002. Targeting CB2 cannabinoid receptors as a novel therapy to treat malignant lymphoblastic disease. Blood 100, 627–634.
Moreno, E., Andradas, C., Medrano, M., Caffarel, M.M., Pérez-Gómez, E., Blasco-Benito, S., Gómez-Cañas, M., Pazos, M.R., Irving, A.J., Carme Lluís Canela, E.I., Fernández-Ruiz, J., Guzmán, M., McCormick, P.J., Sánchez, C., 2014. Targeting CB2-GPR55 receptor heteromers modulates cancer cell signaling. J. Biol. Chem. 289, 21960–21972.
Nafee, N., Schneider, M., Schaefer, U.F., Lehr, C.M., 2009. Relevance of the colloidal stability of chitosan/PLGA nanoparticles on their cytotoxicity profile. Int. J. Pharm. 381, 130–139.
Patel, B., Gupta, V., Ahsan, F., 2012. PEG–PLGA based large porous particles for pulmonary delivery of a highly soluble drug, low molecular weight heparin. J. Controlled Release 162, 310–320.
Parveen, S., Sahoo, S.K., 2011. Long circulating chitosan/PEG blended PLGA nanoparticles for tumor drug delivery. Eur. J. Pharm. 670, 372–383.
Pérez-Artacho, B., Gallardo, V., Ruiz, M.A., Arias, J.L., 2012. Maghemite/poly(D,L-lactide-*co*-glycolyde) composite nanoplatform for therapeutic applications. J. Nanopart. Res. 14, 768–778.
Preet, A., Ganju, R.K., Groopman, J.E., 2008. Δ^9-Tetrahydrocannabinol inhibits epithelial growth factor-induced lung cancer cell migration in vitro as well as its growth and metastasis in vivo. Oncogene 27, 339–346.
Ramer, R., Hinz, B., 2008. Inhibition of cancer cell invasion by cannabinoids via increased expression of tissue inhibitor of matrix metalloproteinases-1. J. Natl. Cancer Inst. 100, 59–69.
Ramer, R., Bublitz, K., Freimuth, N., Merkord, J., Rohde, H., Haustein, M., Borchert, P., Schmuhl, E., Linnebacher, M., Hinz, B., 2012. Cannabidiol inhibits lung cancer cell invasion and metastasis via intercellular adhesion molecule-1. FASEB J. 26, 1535–1548.
Reddy, L.H., Arias, J.L., Nicolas, J., Couvreur, P., 2012. Magnetic nanoparticles: design and characterization, toxicity and biocompatibility, pharmaceutical and biomedical applications. Chem. Rev. 112, 5818–5878.
Sempf, K., Array, T., Gelperina, S., Schorge, T., Meyer, B., Karas, M., Kreuter, J., 2013. Adsorption of plasma proteins on uncoated PLGA nanoparticles. Eur. J. Pharm. Biopharm. 85, 53–60.
Solinas, M., Massi, P., Cinquina, V., Valenti, M., Bolognini, D., Gariboldi, M., Monti, E., Rubino, T., Parolaro, D., 2013. Cannabidiol, a non-psychoactive cannabinoid compound, inhibits proliferation and invasion in U87-MG and T98G glioma cells through a multitarget effect. PLoS One 8, e76918.
Takeda, S., Yamaori, S., Motoya, E., Matsunaga, T., Kimura, T., Yamamoto, I., Watanabe, K., 2008. Δ^9-Tetrahydrocannabinol enhances MCF-7 cell proliferation via cannabinoid receptor-independent signaling. Toxicology 245, 141–146.
Thiele, L., Diederichs, J.E., Reszka, R., Merkle, H.P., Walter, E., 2003. Competitive adsorption of serum proteins at microparticles affects phagocytosis by dendritic cells. Biomaterials 24, 1409–1418.
Traber, M.G., Atkinson, J., 2007. Vitamin E: antioxidant and nothing more. Free Radical Biol. Med. 43, 4–15.
Tran, V.-T., Karam, J.-P., Garric, X., Coudane, J., Benoît, J.-P., Montero-Menei, C.N., Venier-Julienne, M.-C., 2012. Protein-loaded PLGA–PEG–PLGA microspheres: A tool for cell therapy. Eur. J. Pharm. Sci. 45 (1-2), 128–137.
Velasco, G., Sánchez, C., Guzmán, M., 2012. Towards the use of cannabinoids as antitumour agents. Nat. Rev. Cancer 12, 436–444.
Vihola, H., Laukkanen, A., Valtola, L., Tenhu, H., Hirvonen, J., 2005. Cytotoxicity of thermosensitive polymers poly(*N*-isopropylacrylamide), poly(*N*-vinylcaprolactam) and amphiphilically modified poly(*N*-vinylcaprolactam). Biomaterials 26, 3055–3064.